Structure and energetics of a ferroelectric organic crystal of phenazine and chloranilic acid

Kyuho Lee, Brian Kolb, T. Thonhauser, David Vanderbilt, and David C. Langreth

Phys. Rev. B **86**, 104102 — Published 5 September 2012

DOI: 10.1103/PhysRevB.86.104102

Structure and energetics of a ferroelectric organic crystal of phenazine and chloranilic acid

Kyuho Lee,[1,*] Brian Kolb,[2] T. Thonhauser,[2] David Vanderbilt,[1] and David C. Langreth[1,†]

[1] *Department of Physics and Astronomy, Rutgers University, Piscataway, New Jersey 08854, USA*
[2] *Department of Physics, Wake Forest University, Winston-Salem, North Carolina 27109, USA*

We report first-principles calculations for a ferroelectric organic crystal of phenazine and chloranilic acid molecules. Weak intermolecular interactions are properly treated by using a second version of van der Waals density functional known as vdW-DF2 [K. Lee *et al.*, Phys. Rev. B **82**, 081101 (2010)]. Lattice constants, total energies, spontaneous electric polarizations, phonon modes and frequencies, and the energy barrier of proton transfer are calculated and compared with PBE and experiments whenever possible. We show that the donation of one proton from a chloranilic acid molecule to a neighboring phenazine molecule is energetically favorable. This proton transfer is the key structural change that breaks the centrosymmetry and leads to the ferroelectric structure. However, there is no unstable phonon associated with the proton transfer, and an energy barrier of 8 meV is found between the paraelectric and ferroelectric states.

PACS numbers: 61.66.Hq, 71.15.Mb, 77.80.-e, 78.55.Kz

I. INTRODUCTION

Ferroelectric materials are an important class of materials. Their responses to various external stimuli can be used for many applications such as memory devices, electromechanical actuators, ultrasonic sensors, electro-optic devices, and infrared thermal image sensors. Although transition-metal oxides are most widely used for applications, organic ferroelectrics could be attractive alternatives, because they could be non-toxic, flexible, and easy to process.[1] However, ferroelectric organic materials are rare, and substantial efforts are being made to find such materials that could be of practical use.[2] The cocrystal of phenazine (Phz) and chloranilic acid (H_2ca) is one of several recently discovered hydrogen-bonded organic ferroelectrics that have superior crystallinity and properties compared to conventional ferroelectric polymers.[2–13]

The crystal structure of Phz-H_2ca has been determined by X-ray[3,7] and neutron[8] diffraction experiments. The centrosymmetric paraelectric structure (monoclinic $P2_1/n$, $T > T_c = 253$ K) is shown in Fig. 1. There are two molecules of each type (72 atoms in total) per unit cell. The two constituent molecules, Phz and H_2ca, can make hydrogen bonds (H-bonds) with each other, forming linear chains in the crystal. One such chain that runs along the [110] direction in an *ab* plane is shown in Fig. 1(b) as viewed along the *b* and *c* axes (top and bottom subpanels respectively). These chains stack along the *b* direction and fill an *ab* plane, as shown in Fig. 1(c). The next plane above or below [Fig. 1(d)] is, however, filled with chains that run along $[1\bar{1}0]$.

Below 253 K, Phz-H_2ca becomes ferroelectric.[3] In this polar phase (monoclinic $P2_1$), one of the O–H bonds in H_2ca stretches (by about 0.37 Å) toward the N atom in the H-bonded Phz neighbor, adopting the structure shown in Fig. 2(b).[8] (The large arrows in this figure represent the directions of the proton displacements. The other panels will be discussed later in Sec. III.) The polarization, estimated experimentally at 1-2 μC/cm^2, is

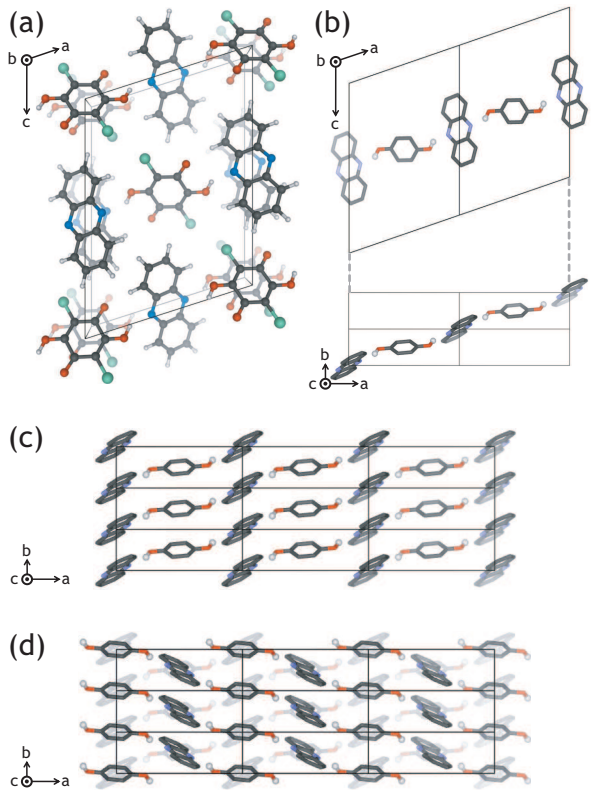

FIG. 1. (Color online) (a) Monoclinic unit cell of the paraelectric structure containing two H_2ca molecules (at body-center and corner sites) and two Phz molecules (at *ab*-face-center and *c*-axis edge-center sites). (b) H-bonded chain of molecules running along [110]. (c) An *ab* plane filled by H-bonded chains running along [110]. (d) Next higher (or lower) *ab* plane filled by H-bonded chains running along $[1\bar{1}0]$. In panels (b-d), all Cl atoms, H atoms bonded to oxygens, and O atoms double-bonded to carbons have been omitted for clarity.

parallel to the b axis because the two-fold screw symmetry cancels out the a and c components of the polarization of each chain.

Interestingly, the proton is found to be almost midway between the nitrogen and oxygen. The observed N–H bond length of 1.41 Å is much larger than the typical value of 1.03 Å in proton-transfered ionic H-bonds.[14] It seems that the proton potential between oxygen and nitrogen has only a single minimum, suggesting that Phz-H_2ca might not be an order-disorder ferroelectric (FE), but rather a displacive-type one, i.e., where the paraelectric (PE) phase has a polar instability associated with a soft phonon mode. However, a dynamic proton fluctuation (i.e., a rapid back-and-forth motion of the proton between two minima located closer to N or O) has been suggested[5] based on nuclear spin relaxation-time measurements using the ^{35}Cl nuclear quadrupole resonance (NQR). The activation-energy barrier for proton transfer is estimated to be 68 meV from the Arrhenius temperature dependence of the fluctuations.[5] Further support for this picture comes from a second ferroelectric phase (FE-II) that appears upon further cooling below 136 K (after passing through an incommensurate phase at 136–146 K). In FE-II, the proton is found to be completely transferred to the Phz nitrogen atom.[7] The observed N–H bond length of 1.12 Å is now consistent with (although a bit longer than) a typical N–H^+ bond length (≈ 1.03 Å) in other organic molecular salts.[14]

In this work, we investigate the structures, energetics, spontaneous electric polarizations, lattice instabilities, and energy barriers for proton transfer by using first-principles calculations. There are two difficulties to a theoretical treatment of this important class of compounds. First, in order to predict stable crystal structures and their properties, it is critical to include quantum mechanical van der Waals interactions (also known as London dispersion interactions), which are important for intermolecular interactions but are missing in conventional exchange-correlation (XC) functionals. Second, because of the small mass of the proton, the proton quantum fluctuations are large enough to significantly affect the relative stabilities of different structures. To address these issues, we use the recently developed van der Waals density functional (vdW-DF2) of Ref. 15 and include the zero-point energy at the harmonic level. The results are compared with experiments as well as with calculations carried out using the semilocal functional of Perdew, Burke, and Ernzerhof (PBE),[16] one of the most successful generalized-gradient functionals. We show that the proton transfer from H_2ca to Phz lowers the energy by 124 meV/unit-cell, and has an energy barrier of 21 meV. No unstable phonon is associated with the proton transfer.

The paper is organized as follows. In Sec. II we describe the details of the computational methods used in the calculations. Then, in Sec. III, we present the results of our calculations of lattice constants, energies, and phonons of polar and nonpolar structures, and of the energy barrier for proton transfer. Finally, we summarize the work in Sec. IV.

II. METHODS

We use the plane-wave pseudopotential method[17] as implemented in the QUANTUM-ESPRESSO package and Troullier-Martins norm-conserving pseudopotentials.[18] We adopt an kinetic-energy cutoff of 80 Ry and a $2\times6\times1$ k-point mesh for the Brillouin-zone sampling. All calculations are done fully self-consistently[19,20] using Soler's efficient algorithm[21] to treat the vdW-DF2 exchange-correlation energy functional. Atomic positions and lattice parameters are fully optimized until the residual forces and stresses are smaller than 7.7 meV/Å and 0.5 kbar, respectively. The Berry-phase technique[22] is used to calculate the polarization of the structures.

The transition path for the proton transfer and its energy profile are determined using the climbing-image nudged elastic band method[23,24] with 7 images. All atoms are relaxed during the process, with the lattice parameters fixed to the experimental equilibrium values for the PE phase.

The zero-point energy corrections are included at the harmonic level using the computed phonon frequencies. For the phonon calculation we use the experimental lattice parameters, the linear-response density-functional perturbation theory[25,26] for PBE, and the finite-difference method for vdW-DF2. The acoustic sum rule is imposed on the force constants. In order to make the phonon frequencies well converged up to 1 cm^{-1}, very tight convergence thresholds are used for the phonon calculation: `tr2_ph` and `conv_thr` are set to 10^{-18} and 10^{-10}, respectively, two orders of magnitude smaller than typical values for inorganic solids.

The FE and PE states have computed DFT energy gaps of 0.5 eV and 1.2 eV, respectively. (Since DFT tends to underestimate gaps, the true gaps are presumably larger.) All bands are fully occupied and there are no unpaired electrons. Thus, Phz-H_2ca is clearly a band insulator, compatible with our choice of methods.

III. RESULTS AND DISCUSSION

A. Lattice constants

First we validate our computational approach by calculating the lattice constants and comparing them with known experimental values as shown in Table I. The vdW-DF2 shows excellent agreement with experiments. For the PE phase, the deviations are 0.00 Å (0%), 0.06 Å (1%), and −0.14 Å (−1%) along a, b, and c, respectively. The relative deviations with respect to the experiments are given in the parenthesis. The deviations for the FE phase are similar: 0.05 Å (0%), 0.09 Å (2%), and −0.27 Å (−2%).

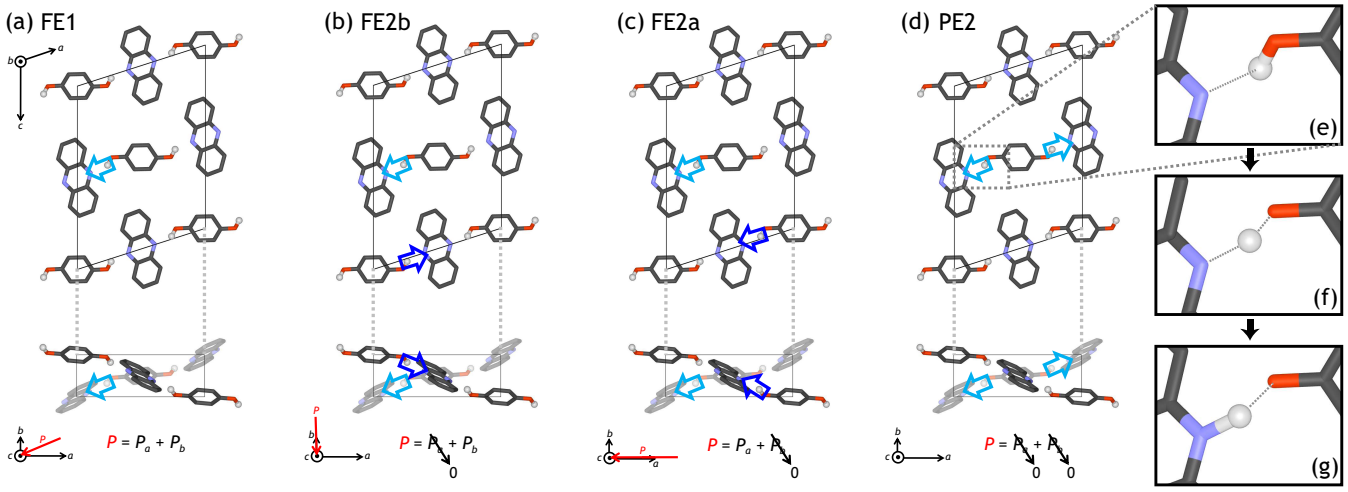

FIG. 2. (Color online) Possible proton transfer (PT) processes in the unit cell, as indicated by large unfilled arrows. (a) Structure FE1, in which a H_2ca donates a proton to a nitrogen in a neighboring Phz, leaving begind an oxygen lone pair on the H_2ca and creating an electric dipole along the PT direction. The direction of polarization P is shown at the bottom left-hand corner as a thin arrow labeled as P; here the PT occurs along $[\bar{1}\bar{1}0]$ so that P has both a and b components. (b) Structure FE2b, in which another PT occurs along $[1\bar{1}0]$ in the other H-bonded chain; P points along b by symmetry. (c) Structure FE2a, in which the second PT occurs along $[\bar{1}10]$ instead; P points along a by symmetry. (d) Structure PE2, a doubly protonated paraelectric structure. (e)-(g) Enlarged view of the PT process.

On the other hand, PBE, which is one of the most successful semi-local functionals, overestimates the PE lattice constants by −0.70 Å (−6%), 1.08 Å (28%) and −0.26 Å (−2%) along a, b, and c axis, respectively [for FE, −0.33 Å (−3%), 0.90 Å (24%) and −0.17 Å (−1%)]. Except for the c lattice constant for the PE phase, all lattice constants are poorly reproduced.

This comparison between vdW-DF2 predictions and experiments confirms that the vdW-DF2 functional is capable of capturing all three important interactions (covalent bonds, H-bonds, and van der Waals interactions) with good fidelity in this organic crystal.

TABLE I. Comparison of experimental lattice constants with those calculated using PBE and vdW-DF2.

Structure	Axis	Lattice constant (Å)		
		Expt.[a]	PBE	vdW-DF2
Paraelectric	a	12.42	11.73	12.42
	b	3.85	4.93	3.90
	c	16.98	16.72	16.84
Ferroelectric	a	12.42	12.10	12.47
	b	3.79	4.69	3.88
	c	16.91	16.74	16.64

[a] [a]Neutron diffraction experiments of Ref. 8, measured at 300 K and 160 K for paraelectric and ferroelectric phase respectively.

B. Proton-transferred structures

In the PE phase, there is no proton transfer and all molecules are neutral. There are two H_2ca molecules per unit cell, and each H_2ca has two hydrogen bonds. The protons in those four hydrogen bonds can be transferred to neighboring Phz molecules. In this section, we consider all the possible proton transfer configurations consistent with the primitive-cell periodicity, starting from the simplest and working toward more complex ones.

The simplest single-proton transfer is shown in Fig. 2(a), where the H_2ca at the center of the unit cell donates a proton to a neighboring Phz (to the left in this figure). The large arrow represents the direction of the proton transfer. We denote the resulting structure as FE1, indicating that it is ferroelectric and only one proton has transferred in the unit cell.

This structural change breaks the centrosymmetry, making it ferroelectric, and lowers the energy by 137 meV per unit cell with respect to the paraelectric phase, which we denote henceforth as PE0. The relative energies of these and other structures (to be discussed shortly) are illustrated in Fig. 3. (All structures and energies in this section are calculated using vdW-DF2. A comparison with PBE will be given later.) The electric polarization P of the FE1 structure points approximately in the [110] direction as is shown by the thin arrow at the bottom left-hand corner of the figure.

The $[H_1ca]^-$ molecule that already donated one proton also has the possibility to donate a second one to the other neighboring Phz in the chain, as shown in Fig. 2(d). We denote this structure as PE2, where the '2' indicates that two protons are transferred in the unit cell. This

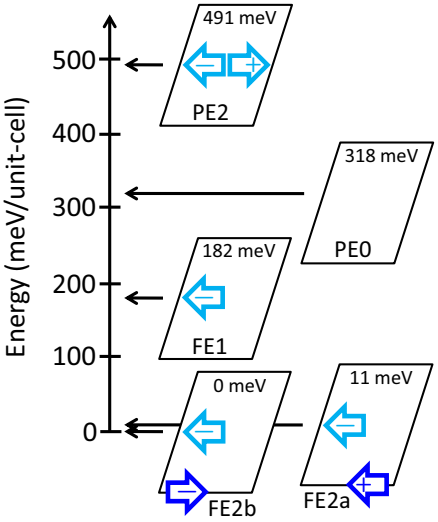

FIG. 3. (Color online) Energies of competitive proton-transferred structures presented relative to the FE2b ground-state energy, which is taken as zero.

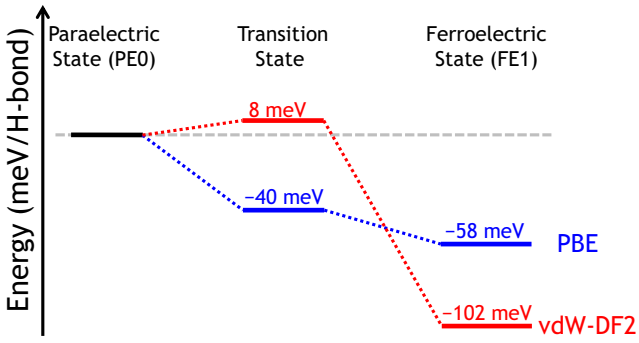

FIG. 4. (Color online) Energies relative to PE0 (left), as calculated with PBE and vdW-DF2, for the transition-state structure leading from PE0 to FE1 (middle) and for FE1 (right). The lattice constants are fixed to experimental values for this comparison, and zero-point energies are included at the harmonic level.

double protonation of a Phz restores the centrosymmetry, so that PE2 has no polarization. However this second proton transfer increases the energy by 309 meV, i.e., the energy of PE2 is 172 meV higher than that of PE. Therefore, in searching for the ground state, we do not consider other configurations based on double-protonation chains, i.e., those involving three (FE3) or four (FE4) transferred protons per cell.

Two possibilities then remain, in which the other H_2ca molecule at the corner site in the figure also donates a proton, as shown in Figs. 2(b-c). We found that the experimental low-temperature ferroelectric structure that we already discussed in detail in the previous section, shown in Fig. 2(b), has the lowest energy of all possible configurations. We now denote it as FE2*b*, indicating that two protons are transferred and the net polarization is parallel to the '*b*' axis. FE2b is more stable than PE0 by 318 meV. This energy reduction is 44 meV larger than twice the PE0-to-FE1 reduction of 137 meV mentioned above. Thus, 44 meV can be taken as an estimate of the interchain coupling strength along *c*.

The polarization of FE2b is calculated to be 4.5 μC/cm^2, in a reasonable agreement with the measured value of $\sim$2 μC/cm^2. Also our calculated N–H bond length of 1.06 Å is consistent with the experimental value of 1.12 Å measured at low temperature in phase FE-II, and with a typical N–H$^+$ bond length of $\approx$1.03 Å in other organic molecular salts.[14] Thus, the structure of the ferroelectric phase agrees also well with experiments.

In the other case, in which the proton is transferred to the left Phz as in Fig. 2(c), only the *a* component of the polarization remains by the symmetry. Following the same notational scheme introduced above, we denote this as FE2*a*. Its energy is only 11 meV/unit-cell higher than that of the ground-state FE2*b* structure.

C. Energy barrier for proton transfer and lattice instability

Here we investigate the proton transfer process from PE0 to FE1 in detail. The transition path for the proton transfer is calculated using the climbing-image nudged elastic band method.[23,24] A close-up view of the initial, transition, and final states of this proton transfer process are shown in Figs. 2(e)-(g). Along the transition path, the two molecules get closer to each other by up to 0.18 Å. They then retreat again as the proton completes its transfer, but not completely; the final proton-transferred pair is closer by 0.05 Å than the initial neutral one.

It is well known that local or semi-local functionals such as PBE underestimate proton-transfer barriers.[27,28] For example, for the intramolecular proton transfer in the malonaldehyde molecule, the energy barrier in PBE is only a quater of the known accurate value of 177 meV (Ref. 27) calculated by the coupled-cluster method with single, double, and perturbative triple exciations [CCSD(T)]. On the other hand, the vdW-DF2 barrier of 183 meV in that case is in excellent agreement with the accurate value, corroborating the validity of our method. We found that the difference between PBE and vdw-DF2 barriers in this molecule can be attributed in roughly equal parts to exchange, correlation, and structural path differences. For the Phz-H_2ca crystal, we found a similar result; our computed PBE barrier of 44 meV from PE0 to FE1 is less than half of the vdW-DF2 value (105 meV). Furthermore, after including the zero-point corrections, the vdW-DF2 barrier drops to 8 meV, and the transition becomes barrierless in PBE as is shown in Fig. 4.

The energetics of proton transfer in vdW-DF2 is in good agreement with experimental observation of the thermally activated proton fluctuation in the high-temperature FE-I phase and the proton-transferred structure in the low-temperature FE-II phase. Also the

apparent single-well proton potential in FE-I could be understood by dynamic proton transfer in a small-barrier double-well potential.

Nevertheless, there could be other pathways not captured by our initial NEB path, or an unstable phonon mode that could trigger the proton displacement toward the FE-I phase. However, our calculation shows that the zone-center phonons of the PE0 structure are all stable. We do not find any unstable mode associated with the proton displacement toward the FE-I phase, the signature of a displacive-type ferroelectric.

Both the proton transfer energetics and the zone-center phonons are in good agreement with experimental observations and support the picture of an order-disorder, as opposed to a displacive, FE transition.

IV. CONCLUSION

By using first-principles density-functional theory, we have studied the structure and energetics of a ferroelectric molecular crystal of phenazine and chloranilic acid, and have analyzed the energy barrier for proton transfer and the stability of lattice vibrational modes. We have shown that the inclusion of van der Waals interactions is crucial for a proper description of this molecular crystal, and that for this case at least, a recently developed vdW-DF2 functional reproduces the structures of the PE and FE phases in good agreement with experiment. We have found that the zone-center phonons of the PE state are all stable, and the proton transfer—the key structural change that leads to the ferroelectric structure—has an energy barrier of 8 meV. The signature of a displacive-type ferroelectric, i.e., lattice instability in the PE phase, has not been found. Accordingly we propose that Phz-H_2ca is an order-disorder FE. Our analysis of the stability of the lattice vibrational modes and the energy barrier for proton transfer supports the possibility that the apparent single-well proton potential in the FE-I phase is an average effect arising from dynamical proton transfer in an asymmetric double-well potential.

ACKNOWLEDGMENTS

We thank K. Rabe, J. H. Lee, A. Kumar, and S. Coh for useful discussions. The work at Rutgers supported by the National Science Foundation under Grant number DMR-0801343.

* Email: klee@physics.rutgers.edu
† Deceased

[1] Z. Hu, M. Tian, B. Nysten, and A. M. Jonas, Nat. Mater. **8**, 62 (2009).
[2] S. Horiuchi and Y. Tokura, Nat. Mater. **7**, 357 (2008).
[3] S. Horiuchi, F. Ishii, R. Kumai, Y. Okimoto, H. Tachibana, N. Nagaosa, and Y. Tokura, Nat. Mater. **4**, 163 (2005).
[4] F. Ishii, N. Nagaosa, Y. Tokura, and K. Terakura, Phys. Rev. B **73**, 212105 (2006).
[5] T. Asaji, K. Gotoh, and J. Watanabe, J. Mol. Struct. **791**, 89 (2006).
[6] K. Saito, M. Amano, Y. Yamamura, T. Tojo, and T. Atake, J. Phys. Soc. Jpn. **75**, 033601 (2006).
[7] K. Gotoh, T. Asaji, and H. Ishida, Acta Crystallogr. C **63**, o17 (2007).
[8] R. Kumai, S. Horiuchi, H. Sagayama, T.-H. Arima, M. Watanabe, Y. Noda, and Y. Tokura, J. Am. Chem. Soc. **129**, 12920 (2007).
[9] S. Horiuchi, R. Kumai, and Y. Tokura, J. Mater. Chem. **19**, 4421 (2009).
[10] J. Fujioka, S. Horiuchi, N. Kida, R. Shimano, and Y. Tokura, Phys. Rev. B **80**, 125134 (2009).
[11] S. Horiuchi, R. Kumai, J. Fujioka, and Y. Tokura, Physica B **405**, S334 (2010).
[12] A. Stroppa, D. Di Sante, S. Horiuchi, Y. Tokura, D. Vanderbilt, and S. Picozzi, Phys. Rev. B **84**, 014101 (2011).
[13] R. Kumai, S. Horiuchi, J. Fujioka, and Y. Tokura, J. Am. Chem. Soc. **134**, 1036 (2012).
[14] F. H. Allen, O. Kennard, D. G. Watson, L. Brammer, A. G. Orpen, and R. Taylor, J. Chem. Soc. Perkin Trans. II , S1 (1987).
[15] K. Lee, E. D. Murray, L. Kong, B. I. Lundqvist, and D. C. Langreth, Phys. Rev. B **82**, 081101 (2010).
[16] J. P. Perdew, K. Burke, and M. Ernzerhof, Phys. Rev. Lett. **77**, 3865 (1996).
[17] J. Ihm, A. Zunger, and M. L. Cohen, J. Phys. C: Solid State Phys. **12**, 4409 (1979).
[18] N. Troullier and J. L. Martins, Phys. Rev. B **43**, 1993 (1991).
[19] T. Thonhauser, V. R. Cooper, S. Li, A. Puzder, P. Hyldgaard, and D. C. Langreth, Phys. Rev. B **76**, 125112 (2007).
[20] D. C. Langreth, B. I. Lundqvist, S. D. Chakarova-Kck, V. R. Cooper, M. Dion, P. Hyldgaard, A. Kelkkanen, J. Kleis, L. Kong, S. Li, P. G. Moses, E. Murray, A. Puzder, H. Rydberg, E. Schrder, and T. Thonhauser, J. Phys.: Condens. Matter **21**, 084203 (2009).
[21] G. Román-Pérez and J. M. Soler, Phys. Rev. Lett. **103**, 096102 (2009).
[22] R. D. King-Smith and D. Vanderbilt, Phys. Rev. B **47**, 1651 (1993).
[23] G. Henkelman, B. P. Uberuaga, and H. Jonsson, J. Chem. Phys. **113**, 9901 (2000).
[24] R. A. Olsen, G. J. Kroes, G. Henkelman, A. Arnaldsson, and H. Jónsson, J. Chem. Phys. **121**, 9776 (2004).
[25] X. Gonze and C. Lee, Phys. Rev. B **55**, 10355 (1997).
[26] S. Baroni, S. de Gironcoli, and A. Dal Corso, Rev. Mod. Phys. **73**, 515 (2001).
[27] S. Sadhukhan, D. Muñoz, C. Adamo, and G. E. Scuseria, Chem. Phys. Lett. **306**, 83 (1999).
[28] Y. Zhao, B. J. Lynch, and D. G. Truhlar, J. Phys. Chem. A **108**, 2715 (2004).